The integration of ZVI-dehalogenation and electrochemical oxidation for the treatment of complex effluents polluted with iodinated compounds

Ángela Moratalla [a], Sergio E. Correia [a], Salvador Cotillas [b,*], Engracia Lacasa [c,*], Pablo Cañizares [a], Manuel A. Rodrigo [a], Cristina Sáez [a]

[a] Department of Chemical Engineering, Faculty of Chemical Sciences and Technologies, University of Castilla-La Mancha, Campus Universitario s/n, 13005 Ciudad Real, Spain
[b] Department of Chemical Engineering and Materials, Faculty of Chemical Sciences, Complutense University of Madrid, Avenida Complutense s/n, 28040 Madrid, Spain
[c] Department of Chemical Engineering, Higher Technical School of Industrial Engineering, University of Castilla-La Mancha, Campus Universitario s/n, 02071 Albacete, Spain

ARTICLE INFO

ABSTRACT

This work evaluates the integration of dehalogenation with Zero Valent Iron (ZVI) and electrochemical oxidation (EO) for the treatment of urines polluted with iodinated X-ray contrast media (ICM). To do this, different strategies were evaluated: pretreatment with ZVI followed by EO (ZVI-EO) or electrolysis enhanced with ZVI-dehalogenation (EO/ZVI). For comparison purposes, single electrolysis was also performed to check the best treatment strategy. Results showed that EO was less efficient than EO/ZVI and ZVI-EO processes. Removal percentages of 74.9%, 87.6% and 99.5% were reached after passing 13.8 Ah dm^{-3} at 10 mA cm^{-2} during EO, EO/ZVI and ZVI-EO, respectively. EO/ZVI process favored the production of large amounts of hydroxyl radicals in the effluent through Fenton's reaction, enhancing the degradation rate of iopamidol (IPM). The pretreatment with ZVI allowed to transform up to 95% of IPM to $C_{17}H_{25}N_3O_8$. Then, electrolysis attained the almost complete removal of the raw pollutant (ZVI-EO). The different iodine species formed at the end of the treatment were also monitored, finding similar proportions of organic iodine species for EO and EO/ZVI processes, although single EO promoted the formation of the stable inorganic iodine (IO_3^-) and EO/ZVI favored the release of I^-. Total organic carbon removal percentages lower than 20% were achieved, suggesting that the technologies employed were selective for the removal of the target pollutant under the operating conditions studied. Finally, the organic IPM by-products were also identified by LC-MS and the chromatographic area profiles showed higher values for EO/ZVI followed by ZVI-EO and EO.

1. Introduction

Iodinated X-ray contrast media (ICM) such as iopromide, iopamidol (IPM), iodixanol, iohexol, iomeprol have been widely used in hospitals to enhance radiological visualization of soft tissues, organs, and blood vessels [1,2]. ICM are administered in high doses, up to 200 g per intravascular administration [2–5] and are excreted in urine [6,7]. In addition, these compounds are characterized by high chemical and biological stability, water solubility and high polarity, making them very difficult to remove effectively by conventional treatments in Waste Water Treatment Plants (WWTP) [8]. Although ICM are non-toxic to the human body, their presence in aquatic environments is considered a major public health concern since they are a source of total absorbable

organic iodine (AOI) and can act as precursors of highly toxic iodine disinfection by-products (I-DBPs) [9–12]. For this reason, the occurrence of ICM in the aquatic environment should be avoided and/or minimized and, hence, it is necessary to develop clean and efficient technologies to remove these organic pollutants before they are discharged into the environment.

In recent years, different technologies have been proposed to remove ICM from ultrapure water, river water, surface water or treated urban wastewater, including conventional processes such as membrane technologies, advanced oxidation processes (AOPs) such as ozonation and ultraviolet irradiation, or chemical processes such as oxidation with persulfate or ferrate [10,13–17]. However, the high investment costs and problems related to cleaning and maintenance of membrane

technologies [18], the formation of I-DBPs or iodinated intermediates compounds [10] have advised against the use of these technologies. Dehalogenation processes with Zero Valent Iron (ZVI) can be an interesting alternative to reduce the concentration of iodinated intermediates generated during the treatment of effluents polluted with ICM. Dong et al. [19] studied the deiodination of IPM by ZVI achieving removal percentages up to 60.8%, but they observed an increase in the amount of I-DBPs after 72 h of treatment. Therefore, this technology does not seem to be enough to solve the problems related to the growing concern about the formation of toxic I-DBPs in treated effluents. On the other hand, electrochemical advanced oxidation processes (EAOPs) have become a promising alternative for the treatment of various emerging pollutants since they present good energy efficiency, high versatility, are environmentally friendly techniques and the energy requirements can be easily solved by using renewable energy [20,21]. Schneider et al. [22] investigated the degradation of different ICMs (iotalamic acid, iopamidol, iohexol, iopromide, iomeprol and diatrizoate) in surface waters and urban treated wastewater (effluents of WWTP) by electrolysis with boron doped diamond (BDD) electrodes. They reported IPM removal efficiencies of 90–100% when applying current intensities within the range 10–25 mA. Similarly, Del Moro et al. [23] studied the electrochemical degradation of different ICMs using two mixed metal oxides (MMO) electrodes at different current densities (64–182 mA cm^{-2}) in the presence of sodium perchlorate or sodium sulphate. They achieved removal percentages around 90–100% with sodium sulfate and complete elimination of ICMs when sodium perchlorate was used as electrolyte. These results confirm the good performance of electrochemical technologies for the removal of iodinated organics, but the studied conditions are far from real wastewaters, and the conclusions obtained must be verified in real effluents or with solutions with compositions that are as real as possible.

With this background, the aim of this work is to integrate the ZVI dehalogenation and electrolysis with MMO anodes for the treatment of hospital effluents in which the presence of ICMs is expected. To do this, the degradation of iopamidol (selected as model of ICM) in complex aqueous matrix (simulating diluted hospital urines) was evaluated using two different treatments: ZVI-pretreatment followed by electrolysis (ZVI-EO) and simultaneous electrolysis and ZVI-dehalogenation (EO/ZVI). For comparison purposes, single ZVI-dehalogenation and electrolysis tests were also carried out. Results are discussed in terms of IPM removal, main transformation products and iodine species formed.

2. Materials and methods

2.1. Chemicals

ZVI (fine granulated, technical grade) was supplied by Panreac (Spain). The target iodinated X-ray contrast media IPM was purchased by Sigma Aldrich (Spain). Uric acid, creatinine, urea, calcium phosphate, diammonium hydrogen phosphate, sodium carbonate, magnesium sulphate and potassium chloride were supplied by Sigma Aldrich (Spain) and used to make the synthetic urine. Sodium carbonate, acetone, nitric acid and 2,6-pyridinedicarboxylic acid (Sigma Aldrich, Spain) were used for the determination of ions concentration. P-dimethylaminobenzaldehyde used as indicator for the measurement of urea in urine matrix was also supplied by Sigma Aldrich (Spain). Other chemicals were analytical grade and supplied from Scharlab. Double deionized water (Millipore Milli-Q system, resistivity: 18.2 MΩ cm at 25 °C) was used to prepare all aqueous solutions.

2.2. Experimental set-up

2.2.1. Single dehalogenation set-up

Single dehalogenation experiments were carried out in closed glass reactors (250 mL). Different ratios of ZVI/IPM were evaluated as 100, 125, 150, 175 and 200, corresponding to ZVI concentrations of 5.00,

Table 1
Synthetic urine composition.

Cl^- (mg dm^{-3})	475.52
PO_4^{3-} (mg dm^{-3})	59.94
SO_4^{2-} (mg dm^{-3})	135.58
CO_3^{2-} (mg dm^{-3})	94.35
Na^+ (mg dm^{-3})	72.34
K^+ (mg dm^{-3})	524.45
NH_4^+ (mg dm^{-3})	22.72
Ca^{2+} (mg dm^{-3})	10.99
Mg^{2+} (mg dm^{-3})	34.33
Iopamidol (mg dm^{-3})	50.00
Urea (mg dm^{-3})	3333.33
Creatinine (mg dm^{-3})	166.67
Uric acid (mg dm^{-3})	50.00
pH	5.8

6.25, 7.50, 8.75 and 10.00 g dm^{-3}, respectively. In each test, 200 mL of urine polluted with 50 mg dm^{-3} of IPM, and different doses of ZVI was shaken at 150 rpm using a Thermo MaxQ 2000 Orbital Shaker. The temperature was kept constant at 30 ºC and the initial pH of the samples was 6.0. The duration of each test was 146 h. The composition of the synthetic urine employed in this work is shown in Table 1 [24].

2.2.2. Electrochemical set-ups: single and combined with ZVI

Three different electrochemical set-ups were tested: (1) EO, 2) ZVI-EO and 3) EO/ZVI as shown in Fig. S1. The EO process was carried out in a bench-scale plant by using a MicroFluidic Flow-Through cell (MF-FT). Further mechanic details of the MF-FT cell are provided elsewhere [25]. 3D $MMO/IrO_2Ta_2O_5$ supplied by Tianode® and a perforate-plate stainless steel AISI 304 were used as anode and cathode, respectively. The surface area (49.5 cm^2) was estimated by determining the surface/geometric area ratio [26]. The interelectrode gap between both electrodes was 150 μm. The system temperature was set at 30 ºC using a heat exchanger. The ZVI-EO process consists of a pretreatment with ZVI for 146 h followed by an electrolysis treatment. In the ZVI-pretreatment step, the solution was filtered at the end of the experiment with 0.45 μm Nylon filters to avoid the iron suspended particles and then, it was introduced into electrolysis set-up. Finally, the EO/ZVI process was carried out coupling a fluidised bed with ZVI to the MF-FT cell. In all electrochemical tests, the current density applied was 10 mA cm^{-2} and the operation time was 74.5 h.

2.3. Analytical procedures

IPM was monitored and quantified by HPLC (Jasco 2080 Plus coupled a DAD detector) using a Zorbax Eclipse Plus C-18 column (4.6 mm x 100 mm; 3.5 μm). The mobile phase consisted of 13% methanol and 87% aqueous solution with 0.1% formic acid, using a flow rate of 0.1 mL min^{-1}. The UV detector was set at 240 nm, the injection volume was 20 μL and the column temperature was set to 25 ºC. Uric acid was also measured by HPLC using the same equipment. In this case, a Hi-Plex H column (4.6 mm x 100 mm; 3.5 μm) was used. The mobile phase consisted of 5 mM H_2SO_4. The DAD detection wavelength was 210 nm and the injection volume was 20 μL.

An Agilent 1260 series HPLC Infinity coupled to an Agilent time-of-flight mass spectrometer (LC-MS TOF 6320) was used to identify IPM intermediate compounds. It was operated in electrospray positive ionization (ESI) mode. Capillary, nebulizer, drying gas, gas temperature and skimmer voltage were 3500 V, 50 psi, 10 L min^{-1}, 325 ºC and 65 V, respectively. Chromatographic separation of target IPM intermediates was achieved at 25 ºC. The mobile phase consisted of formic acid 0.1% (A), acetonitrile (B) and methanol (C). The gradient programming was as follows: 1) 86% (A), 1% (B) and 13% (C) for 16 min, 2) 69% (A), 30% (B) and 1% (C) for 6.5 min and 3) 86% (A), 1% (B) and 13% (C) for 12.5 min. The injection volume was 20 μL and the flow rate set at 0.1 mL min^{-1} using a Zorbax Eclipse Plus C-18 column.
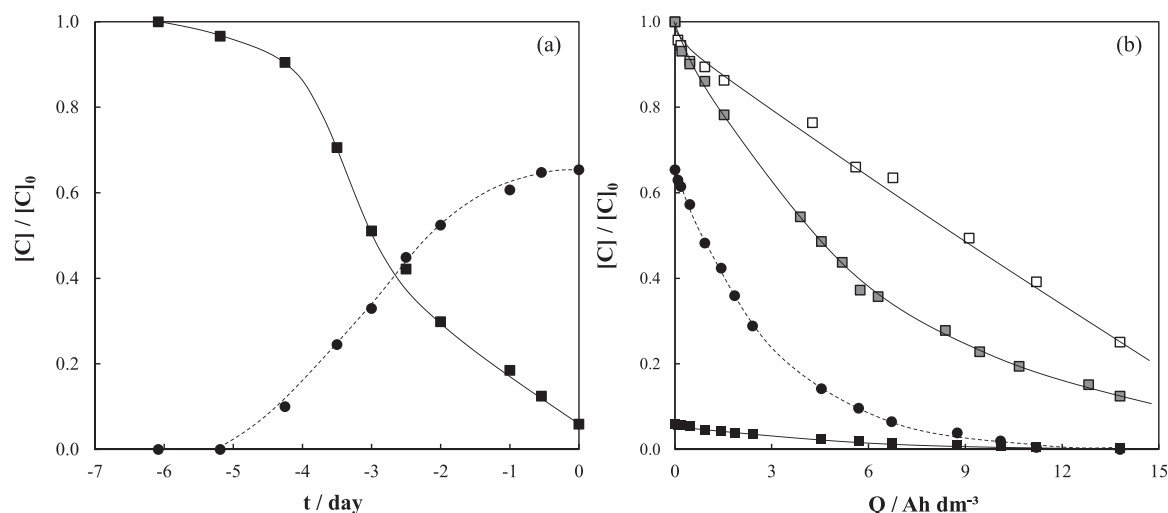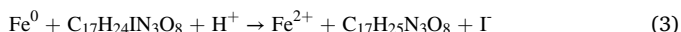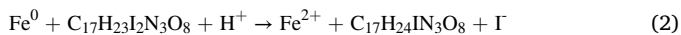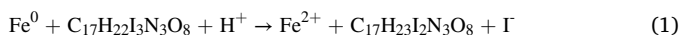
Fig. 1. (a) Evolution of IPM during the ZVI-pretreatment of hospital urine with ZVI/IPM ratio of 150; (b) Evolution of IPM and its main dehalogenation product during the electrochemical processes: (□) EO, (▨) EO/ZVI, (■) ZVI-EO, (●) $C_{17}H_{25}N_3O_8$. $[IPM]_o = 50$ mg dm^{-3} , $j = 10$ mA cm^{-2}.

Iodide, iodate and other anions present in the effluent were monitored by ion chromatography (IC) using a Metrohm 930 Compact IC Flex coupled to a conductivity detector using a Metrosep A Supp 7 column. Creatinine and other cations were also analyzed by IC using a Metrosep A Supp 4 column. The mobile phase consisted of 85:15 v/v 3.6 mM Na_2CO_3/Acetone solution for the determination of anions and 1.7 mM HNO_3 and 1.7 mM 2,6-pyridinedicarboxylic acid solution for the determination of cations. The urea concentration was measured by spectrophotometric method using a UV-1700 Shimadzu Spectrophotometer, according to previously reported methodologies [27]. Total Organic Carbon (TOC) was monitored using a Multi N/C 3100 Analytik Jena Analyzer. Total oxidants were determined iodometrically according to standard methods reported in literature [28].

3. Results and discussion

Fig. 1 shows the evolution of IPM in urine media for the different electrochemical treatment strategies assessed: (1) EO, (2) ZVI-EO and (3) EO/ZVI. The ZVI/IPM ratio was fixed from preliminary dehalogenation tests carried out using values of 100, 125, 150, 175 and 200 (Fig. S2). As observed, after 146 h the deiodination percentages were 83.56%, 86.12%, 94.10%, 97.92% and 98.00% for ZVI/IPM ratios of 100, 125, 150, 175 and 200, respectively. As reported in literature [29, 30], the higher the ZVI/IPM ratio the higher the IPM deiodination percentages since higher ZVI amounts mean larger available surface areas to develop redox reactions.

The IPM deiodination along the ZVI-pretreatment could take place partially (Eqs. 1–2) to form $C_{17}H_{23}I_2N_3O_8$ (M1) or $C_{17}H_{24}IN_3O_8$ (M2), or completely (Eq. 3) to be transformed into the fully deiodinated $C_{17}H_{25}N_3O_8$ (M3), which was the main deiodinated product detected in all tests.

$$Fe^0 + C_{17}H_{22}I_3N_3O_8 + H^+ \rightarrow Fe^{2+} + C_{17}H_{23}I_2N_3O_8 + I^- \quad (1)$$

$$Fe^0 + C_{17}H_{23}I_2N_3O_8 + H^+ \rightarrow Fe^{2+} + C_{17}H_{24}IN_3O_8 + I^- \quad (2)$$

$$Fe^0 + C_{17}H_{24}IN_3O_8 + H^+ \rightarrow Fe^{2+} + C_{17}H_{25}N_3O_8 + I^- \quad (3)$$

Bearing in mind these results, the ZVI/IPM ratio of 150 was chosen to carry out the ZVI-EO and EO/ZVI treatments since the IPM deiodination percentage was almost 95% and it would increase less than 5% by adding much more quantity of ZVI. Fig. 1a shows the evolution of IPM and of $C_{17}H_{25}N_3O_8$ (M3) during the ZVI-dehalogenation with ZVI/IPM ratio of 150, while part b of Fig. 1 shows the variation of both during the following electrolysis with MMO electrodes at 10 mA cm^{-2} of current
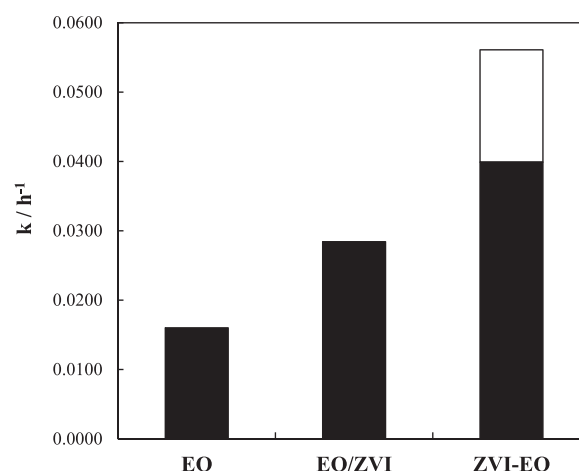
Fig. 2. Kinetic constants for the different electrochemical treatment strategies proposed for the removal of IPM from urine. (■) Electrochemical treatment; (□) ZVI-pretreatment.

density. For comparison purpose, Fig. 1b also shows the evolution of IPM concentration during EO/ZVI and the EO.

As can be seen, the ZVI-pretreatment of hospital urine containing 50 mg dm^{-3} IPM with a ZVI/IPM ratio of 150 along 6 days allowed to decrease the IPM concentration below 95% and at the same time, primarily promoted the fully deiodination of IPM to $C_{17}H_{25}N_3O_8$. Indeed, 24 mg dm^{-3} of $C_{17}H_{25}N_3O_8$ remained in solution which were totally removed during the EO process for an applied electric charge of 13.8 A h dm^{-3}. The least efficient treatment strategy was the single EO process which only attained an IPM removal percentage of 74.9% for an applied electric charge of 13.8 A h dm^{-3}. The combination of EO with ZVI particles (EO/ZVI) seems to enhance the removal efficiencies of IPM from urine media. The ZVI particles are widely known to degrade chlorinated volatile organic compounds via hydrogenolysis and dihaloelimination. Hydrogenolysis involves a carbon-carbon or carbon-heteroatom bond cleavage and the replacement of the chlorine anion by hydrogen cation along with an addition of two electrons. Dihaloelimination is based on the elimination of pairs of Cl atoms without the addition of hydrogen or electrons just by forming on adjacent carbons an additional C–C bond often termed as β-elimination [31,32]. However, ZVI particles have been poorly tested for the reductive elimination of other halogens such as iodine within organic compounds [33,34]. The
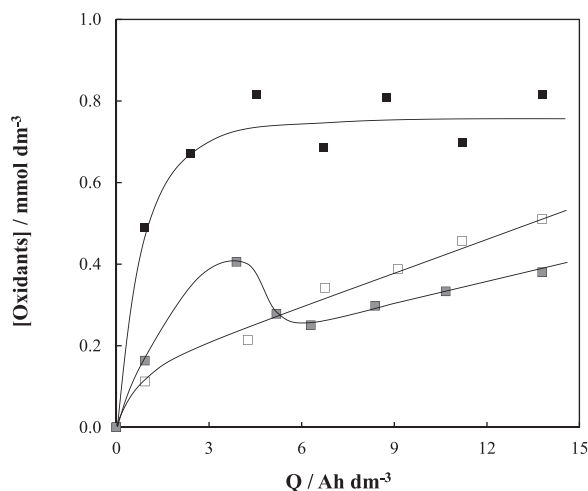
Fig. 3. Concentration of electrogenerated oxidants as a function of applied electrical charge during EO (□), EO/ZVI (▨) and ZVI-EO (■) processes.

removal of IPM can be observed to increase till 87.6% when the treated solution from the EO process passed through a fluidised bed of ZVI particles as shown in Fig. 1 (EO/ZVI). However, an almost complete degradation of IPM was reached when a ZVI-pretreatment was carried out.

Experimental data from the electrolysis of urine were fitted to a first-order kinetic model (Eq. 4), obtaining correlation values above 0.9781. The resulting kinetic constants (k) for the different electrochemical treatment strategies tested are plotted in Fig. 2.

$$Ln\,(C_0/C) = k \cdot t \tag{4}$$

The electrochemical treatment strategy to remove IPM from urine media significantly influences the kinetic constant values of the electrochemical process. Single EO process attained a kinetic constant value of 0.0160 h^{-1} which increased more than two-folds (k = 0.0284 h^{-1}) for the EO/ZVI process. Additionally, the IPM removal was even faster (k = 0.0399 h^{-1}) during the ZVI-EO treatment although it is important to notice that the IPM concentration was reduced almost 95% (2.91 mg dm^{-3}) before the electrochemical treatment. Then, the use of ZVI as pretreatment (ZVI-EO) or combined with EO process (EO/ZVI) greatly improved the kinetics of the IPM degradation reaction. These results suggest that the presence of ZVI during the electrochemical

treatment of urine improves the removal of IPM in terms of efficacy (applied electric charge) and kinetics (time). The kinetic constants calculated for IPM removal are lower than the data reported in the literature related to the degradation of this compound by electrochemical technologies [22,23]. However, the electrode material used, and the operating conditions are very different, applying higher current densities (about 100 mA cm^{-2}) and Boron Doped Diamond electrode.

The enhancement in the removal of IPM by combining electrolysis and dehalogenation with ZVI was also expected to be reflected in a different evolution of electrogenerated oxidants. These species were formed mainly from the oxidation of the inorganic salts contained in the urine (1000 mg dm^{-3} of potassium chloride, 170 mg dm^{-3} of magnesium sulfate, 166.67 mg dm^{-3} of sodium carbonate, 83.34 mg dm^{-3} of diammonium hydrogen phosphate and 28.34 mg dm^{-3} of calcium phosphate) [35,36]. The oxidation of these inorganic species led to the formation of a cocktail of oxidants such as hypochlorite, persulfate, peroxodiphosphate and/or percarbonates [37]. Fig. 3 shows the evolution of the concentration of the total oxidants monitored during the three electrochemical processes studied. It is important to remark that the concentration plotted is not referred to the total generated oxidants but to the oxidants that had not reacted and still remained in the bulk solution.

As can be observed, the concentration of total oxidants increased with the applied electric charge for all the tests performed, however, the trends were quite different depending on the treatment strategy evaluated. Specifically, the monitored oxidants were almost linearly increasing up to 0.511 mmol dm^{-3} during the single EO process whereas this concentration sharply increased to reach a plateau zone at 0.750 mmol dm^{-3} for the ZVI-EO process. This fact could be primarily explained by the different initial IPM concentration in urine (50 mg dm^{-3} *vs.* 3 mg dm^{-3}) since the ZVI-pretreatment allowed to decrease up to 95% of IPM concentration. In this case, the amount of oxidants required to remove IPM and other related oxidation products is lower and, hence, the concentration of these species remaining free in the effluent is higher. On the other hand, the oxidants reached a maximum concentration of 0.405 mmol dm^{-3} at 3.89 Ah dm^{-3} during the combined EO/ZVI process and after that, the concentration decreased below 0.300 mmol dm^{-3} to linearly increases later up to 0.380 mmol dm^{-3}, following a similar profile than single EO process. Hence, three different zones can be distinguished in the concentration of oxidants during the hybrid EO/ZVI process: initial increase (electro-oxidation of the ions naturally contained in urine), intermediate decrease (consumption of oxidants in the degradation of organics) and final increase. This last behavior could be related to the presence of ZVI
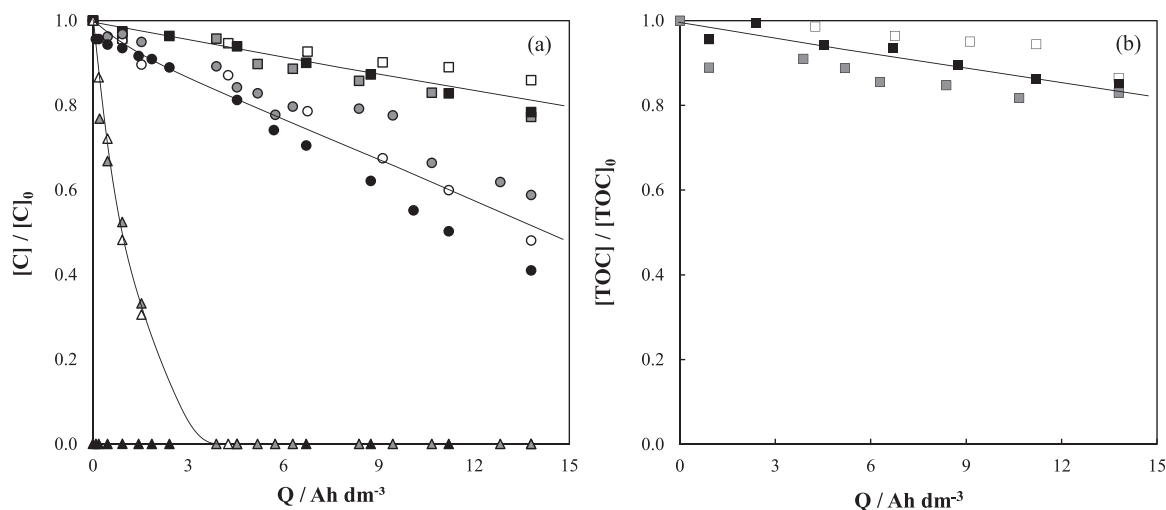
Fig. 4. Evolution of organic compounds (a) and TOC (b) with the applied electrical charge during the treatment of urine polluted with IPM by different electrochemical processes. (square) urea, (circle) creatinine, (triangle) uric acid. White symbols: EO, gray symbols: EO/ZVI, black symbols: ZVI-EO.
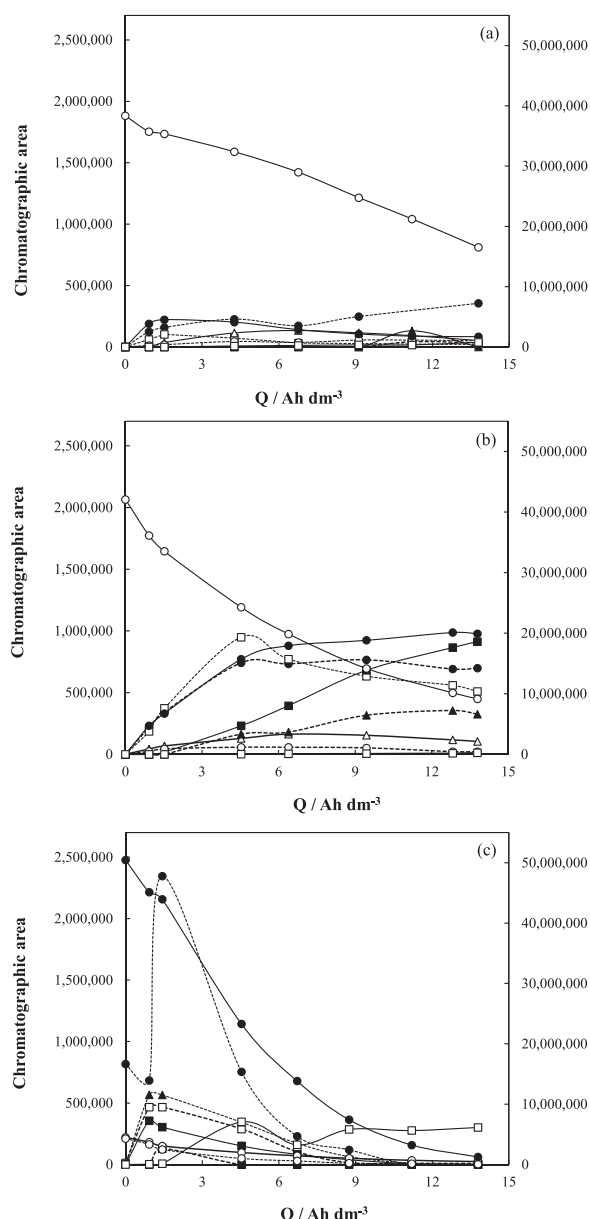
Fig. 5. Evolution of different organic derivates (expressed in terms of chromatographic area) with the applied electric charge during the removal of IPM in urine applying different treatment strategies. Treatment strategies: a) EO process, b) EO/ZVI process, c) ZVI-EO process. Initial organic compound: ──⬤── –○–IPM (secondary axis). Organic intermediates detected: –○–M1 (secondary axis), –●–M2, –●–M3 (secondary axis), –▢–M5, –▢–M10 (secondary axis), –■–M15, –△–M18, –▲–M20, –▲–M23, –■–M25.

particles during the EO process since according to Eq. 5, ZVI can degrade and oxidize organic compounds in the presence of dissolved oxygen where ZVI transfers two electrons to O_2 to produce H_2O_2 [32]. The produced H_2O_2 can be reduced to H_2O by another two-electron transfer from ZVI (Eq. 6) and therefore, the combination of H_2O_2 and Fe^{2+} can produce hydroxyl radicals (•OH) (Eq. 7) which possess a strong oxidizing capacity.

$$Fe^0 + O_2 + 2H^+ \rightarrow Fe^{2+} + H_2O_2 \tag{5}$$

$$Fe^0 + H_2O_2 + 2H^+ \rightarrow Fe^{2+} + 2H_2O \tag{6}$$

$$Fe^{2+} + H_2O_2 \rightarrow Fe^{3+} + \cdot OH + OH^- \tag{7}$$

The formation of these oxidizing species may attack not only the IPM

but also other organic compounds that are naturally contained in urine such as urea (3333.33 mg dm^{-3}), creatinine (166.67 mg dm^{-3}) and uric acid (50.00 mg dm^{-3}), promoting their complete mineralization [38]. Fig. 4a shows the evolution of these organic compounds and Fig. 4b plots the evolution of TOC during the different treatment strategies tested.

Uric acid reached 100% elimination for all cases, and it could even be eliminated during the ZVI-pretreatment. This compound had the lowest initial concentration of all the organics presented in urine (50 mg dm^{-3}) and it presents a molecular structure typical of a polycyclic compound which is easier to attack [39]. Furthermore, uric acid is a photosensitive compound which can be easily degraded by sunlight. On the other hand, 17.6% of the creatinine was also degraded during the ZVI-pretreatment process and then, its degradation increased up to 60% at 13.80 Ah dm^{-3} after the electrochemical process (ZVI-EO). Opposite to that, the removal percentage of creatinine remained at 41.2% during combined EO/ZVI process and slightly increased until 52.0% for the single EO process. Finally, the evolution of urea linearly decreased with the applied electric charge although the reduction percentages only ranged from 14.1% to 22.7%. Single EO was the less efficient process for urea degradation whereas the combined EO/ZVI process was the most efficient since the simultaneous presence of ZVI particles during the EO process may lead to the development of the Fenton's reaction as previously described (Eqs. 5–7). Furthermore, the evolution of urea strongly conditioned the performance of TOC monitored (Fig. 4b), since was the organic compound with the highest concentration in urine. TOC decay followed a linear decrease to attain degradation percentages of 13.5%, 15.0% and 17.0% for single EO, ZVI-EO and EO/ZVI processes, respectively. This fact demonstrates that single or combined electrolysis may be promising alternatives to reduce the chemical risk of polluted water since they are highly selective in the degradation of target pollutants like IPM even in complex water matrices such as urine [24,37].

For comparison purposes, Table S1 summarizes different treatment technologies employed for the degradation of IPM. The comparison of these results is not easy because the performance of IPM degradation should not only depend on the treatment technology but also on water composition, initial concentration of IPM and many other additional factors. However, it can be seen that electrochemical technologies allow to completely remove IPM from simple matrixes. Furthermore, it is important to highlight that the integration of electrolysis and ZVI-dehalogenation proposed in this work attains removal efficiencies close to 100% using MMO anodes and very low current densities. This reveals that the energy requirements for removing IPM form complex matrixes can be reduced by the combined process.

To shed light on the possible intermediate organic compounds generated from the removal of IPM, Fig. 5 shows the LC-MS identification profile and concentration (expressed in terms of chromatographic area) of the organics detected during the different processes evaluated: EO (Fig. 5a), EO/ZVI (Fig. 5b), ZVI-EO (Fig. 5c). Likewise, these profiles were compared with the evolution of the chromatographic area related to the IPM.

As can be observed, more than twenty intermediates were detected by LC-MS during the removal of IPM regardless the treatment strategy tested. Specifically, fifteen transformation products were identified for the ZVI-EO process whereas nineteen and twenty-two intermediates were identified in during EO and EO/ZVI, respectively. However, the profiles of the organics followed different behaviors depending on the treatment developed. EO presented the lowest chromatographic areas followed by the ZVI-EO and EO/ZVI. The nature of the different transformation products suggests that IPM ($m/z = 777.8541$) is degraded to M1 ($m/z = 650.9575$), M2 ($m/z = 525.0608$) and M3 ($m/z = 399.6420$) through the loss of one, two or three iodine atoms from the benzoic ring (partial and / or total dehalogenation process) (Eqs. 1–3). The chromatographic areas of these dehalogenated products (M1, M2 and M3) were much more significant in EO/ZVI and ZVI-EO.

On the other hand, the intermediate products M4 ($m/z = 666.9524$), M5 ($m/z = 415.1591$), M6 ($m/z = 431.1540$) and M7 ($m/z = 447.1489$)
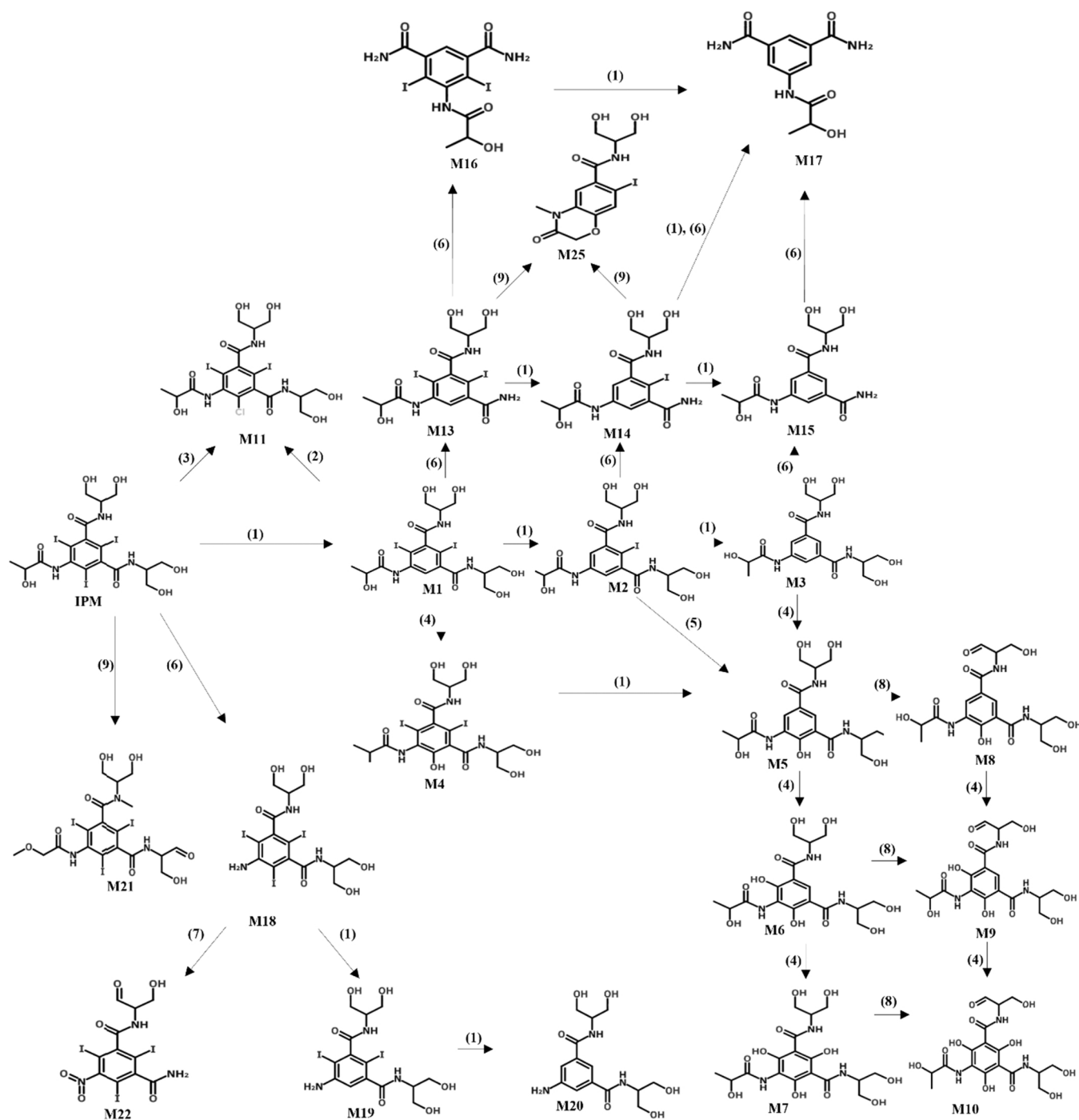
Fig. 6. Possible degradation pathway of IPM by EO/ZVI process. (1) deiodination, (2) addition of Cl, (3) substitution of I by Cl, (4) hydroxyl addition, (5) substitution of I by hydroxyl, (6) amide hydrolysis, (7) amino oxidation, (8) hydrogen abstraction, (9) other processes.

may be generated from the addition of hydroxyl radicals during the EO/ZVI process as shown in Eq. 7. Likewise, M5, M6 and M7 can experience a process of dehydrogenation or hydrogen abstraction promoting the transformation products M8 ($m/z = 413.1434$), M9 ($m/z = 429.1383$) and M10 ($m/z = 445.1333$), respectively. In addition, various transformation products may be generated through the amide hydrolysis in a C-N in the side chains of the molecule that have two alcohol groups, such as M13 ($m/z = 576.9207$), M14 ($m/z = 451.0240$) and M15 ($m/z = 325.1274$) from M1, M2 and M3, respectively. Similarly, M15 can be generated from M14, and the latter from M13 by a process of dehalogenation (substitution of an iodine atom of the benzoic ring). Additionally, M13, M14 and M15 may produce M16 ($m/z = 502.8839$) and

M17 ($m/z = 251.0906$) by the hydrolysis of another amide group. Furthermore, the by-products M18 ($m/z = 704.8330$), M19 ($m/z = 578.9363$) and M20 ($m/z = 327.1430$) may be produced due to the amide hydrolysis in a C-N bond in the side chain formed by a group alcohol and a methyl group. Various by-products with the -NO$_2$ group were also detected in the compounds M22 ($m/z = 658.7547$), M23 ($m/z = 460.8369$) and M24 ($m/z = 209.0437$) from the amino oxidation processes. Other by-products were also identified as M21 ($m/z = 778.8541$) and M25 ($m/z = 406.0026$). Finally, the complex composition of the urine media also influenced on the generation of intermediate products due to the presence of chloride ions. Then, M11 ($m/z = 684.9185$) and M12 ($m/z = 433.1252$) were detected as a
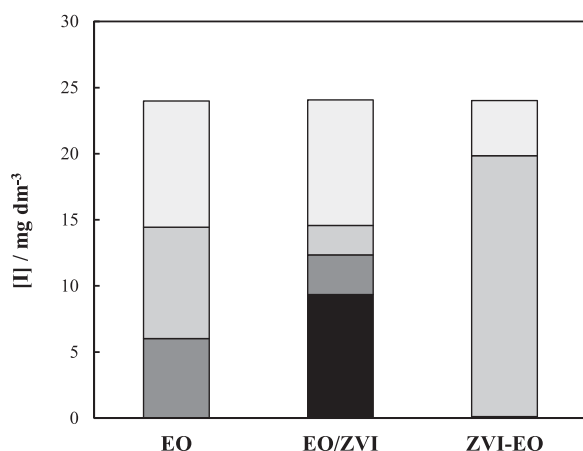
Fig. 7. Iodine speciation in treated urine after passing 13.8 Ah dm^{-3}. (■) [I-I^{-}], (■) [I-IO$_3^{-}$], (■) [I-IPM] and (■) [I-ITP].

consequence of adding Cl in M1, M2 or M3 and/or substituting an iodine atom for a Cl atom in IPM during the EO and EO/ZVI processes. More information about all intermediates found during the degradation of IPM is shown in Table S2 (supplementary material).

In literature, some IPM derivates have already been monitored during the treatment of IPM by AOPs such as ozone/peroxymonosulfate, UV-LED/chlorine [11] or Fe (II) activated by persulfate [16]. Herein, many of the by-products identified in this research were consistent with those found in the literature. Fig. 6 shows a possible degradation pathway for IPM by EO/ZVI process. Furthermore, degradation pathways for IPM removal by ZVI-EO and single EO processes have been included as supplementary material (Figs. S3 and S4, respectively).

On the other hand, it is very important to estimate the amount of iodine release from IPM since it could act as a precursor to form highly toxic iodinated disinfection by-products (I-DBP) that present a much higher toxicity than brominated or chlorinated analogues [40,41]. The reduction of iodinated organic compounds using ZVI has been reported to follow two different mechanisms including direct and indirect reductions [33,42,43]. The direct reduction takes place after the formation of a chemisorption complex (Eqs. 8–9) or by electron tunneling to the physically adsorbed compound which is separated from the iron surface by adsorbed water or an oxide film. The indirect reduction is carried out as a reaction of the organic compounds with adsorbed atomic hydrogen (H$_{ads}$) by the formation of chemisorbed hydride complexes (Eqs. 10–11).

$$Fe^0 + RI + H^+ \rightarrow Fe^{2+} + RH + I^- \tag{8}$$

$$2Fe^{2+} + RI + H^+ \rightarrow 2Fe^{3+} + RH + I^- \tag{9}$$

$$Fe^0 + 2H^+ \rightarrow Fe^{2+} + 2H_{ads} \tag{10}$$
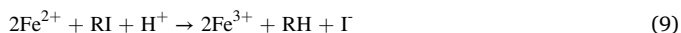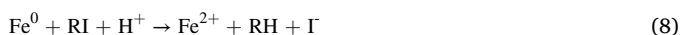
$$2H_{ads} + RI \rightarrow H^+ + RH + I^- \tag{11}$$

Fig. 7 shows the concentration of iodine detected in the bulk solution at the end of each treatment evaluated. The plotted iodine concentrations were analysed by IC as iodine from iodide ([I-I^{-}]$_t$) or iodate ([I-IO$_3^{-}$]$_t$), by HPLC as the iodine immersed in the remained IPM ([I-IPM]$_t$) or by a mass balance as the iodine from other organic derivatives ([I-ITP]$_t$) according to Eq. (12). At this point, it is noticeable that the theoretical total iodine concentration in solution was 24.5 mg dm^{-3} coming from the 50 mg dm^{-3} of IPM in urine. Additionally, [I-IPM]$_t$ values were known to be 6.02, 3.00 and 0.06 from EO, ZVI-EO and PT-EO processes observed in Fig. 1b, respectively.

$$[I]_{Total} = [I\text{-}IPM]_0 = [I\text{-}IPM]_t + [I\text{-}I^{-}]_t + [I\text{-}IO_3^{-}]_t + [I\text{-}ITP]_t \tag{12}$$

As observed, 9.35 and 0.07 mg dm^{-3} I-I^{-} remained in solution after EO/ZVI and ZVI-EO processes, respectively, because the release of iodide was induced by both direct and indirect reductions of IPM by ZVI as

shown in Eqs. 8–11. Iodide has been reported to be easily oxidized to hypoiodous acid (HIO) or hypoiodite (IO^{-}) under the presence of ozone, chlorine or chloramines during disinfection processes and thus, these species may react with natural organic matter contained in solution to form I-DBPs, such as iodinated trihalomethanes [10,44]. Conversely, the electrochemical oxidation process may transform iodide into iodate which has been reported to decrease the formation of I-DBPs due to its high stability [45]. The final concentrations of iodate were 2.23, 8.42 and 19.73 mg dm^{-3} following the efficiency order of treatments EO/ZVI < EO < ZVI-EO. This fact means that the 95% of the dehalogenated IPM during ZVI-pretreatment led to the release of iodide (Eqs. 8–11) which was later oxidized mainly to the stable iodate during ZVI-EO. Indeed, the ZVI-EO process attained 9-times higher iodate concentrations than the combined EO/ZVI due to the early availability of release iodide in electrochemical treated solution. Likewise, the ZVI-pretreatment allowed to obtain the lowest concentration of [I-ITP]$_t$ since the organic iodine content during ZVI-EO process was 4.17 mg dm^{-3} in comparison with its concentration in EO and EO/ZVI treated effluents: 9.55 and 9.46 mg dm^{-3}, respectively.

4. Conclusions

From this work, the following conclusions can be drawn:

- The combined electrolysis and dehalogenation with ZVI process improves both the efficiency and the kinetics of the single electrochemical process to degrade IPM from urine due to the promotion of higher concentrations of oxidizing species. Nevertheless, the almost complete removal of IPM is only attained with the ZVI-EO strategy.
- Single electrolysis leads mainly to the equal formation of both stable inorganic iodine (iodate) and organic iodine species. On the other hand, EO/ZVI process promotes the release of iodide in solution which could formed undesirable I-DBPs and it also encourages a similar concentration of organic iodine species. Finally, the ZVI-EO process attains the highest promotion of inorganic iodine species in the final solution with 0.07 mg dm^{-3} of iodide, 19.73 mg dm^{-3} of iodate and the lowest proportion of organic iodine species.
- The organic IPM by-products were identified by a LC-MS. Fifteen organic derivates were identified for the ZVI-EO process, nineteen for single EO and twenty-two for the combined EO/ZVI. Nevertheless, the chromatographic area profiles show higher values for EO/ZVI follows by ZVI-EO and EO.

CRediT authorship contribution statement

Declaration of Competing Interest

Acknowledgements

Appendix A. Supporting information

Supplementary data associated with this article can be found in the online version at doi:10.1016/j.jece.2022.107587.

References

[1] C. Yangin-Gomec, T. Olmez-Hanci, I. Arslan-Alaton, S. Khoei, H. Fakhri, Iopamidol degradation with ZVI- and ZVA-activated chemical oxidation: Investigation of toxicity, anaerobic inhibition and microbial communities, J. Environ. Chem. Eng. 6 (6) (2018) 7318–7326, https://doi.org/10.1016/j.jece.2018.09.028.

[2] A. Nowak, G. Pacek, A. Mrozik, Transformation and ecotoxicological effects of iodinated X-ray contrast media, Rev. Environ. Sci. Bio/Technol. 19 (2) (2020) 337–354, https://doi.org/10.1007/s11157-020-09534-0.

[3] I. Arslan-Alaton, T. Olmez-Hanci, G. Korkmaz, C. Sahin, Removal of iopamidol, an iodinated X-ray contrast medium, by zero-valent aluminum-activated H2O2 and S2O82−, Chem. Eng. J. 318 (2017) 64–75, https://doi.org/10.1016/j.cej.2016.05.021.

[4] C. Christiansen, X-ray contrast media–an overview, Toxicology 209 (2) (2005) 185–187, https://doi.org/10.1016/j.tox.2004.12.020.

[5] S. Iwano, S. Kamiya, R. Ito, S. Nakamura, S. Naganawa, Iodine-related attenuation in contrast-enhanced dual-energy computed tomography in small-sized solid-type lung cancers is associated with the postoperative prognosis, Cancer Imaging 21 (1) (2021) 7, https://doi.org/10.1186/s40644-020-00368-1.

[6] I. Arslan-Alaton, O. Kolba, T. Olmez-Hanci, Removal of an X-Ray contrast chemical from tertiary treated wastewater: Investigation of persulfate-mediated photochemical treatment systems, Catal. Today 313 (2018) 134–141, https://doi.org/10.1016/j.cattod.2017.11.002.

[7] S. Pérez, D. Barceló, Fate and occurrence of X-ray contrast media in the environment, Anal. Bioanal. Chem. 387 (4) (2007) 1235–1246, https://doi.org/10.1007/s00216-006-0953-9.

[8] B. Ning, N.J.D. Graham, P.D. Lickiss, Degradation of X-ray contrast media compounds by combined ozone and ultrasound, Water Environ. Res. 79 (12) (2007) 2427–2436, https://doi.org/10.2175/106143007×212120.

[9] S.E. Duirk, C. Lindell, C.C. Cornelison, J. Kormos, T.A. Ternes, M. Attene-Ramos, J. Osiol, E.D. Wagner, M.J. Plewa, S.D. Richardson, Formation of toxic iodinated disinfection by-products from compounds used in medical imaging, Environ. Sci. Technol. 45 (16) (2011) 6845–6854, https://doi.org/10.1021/es200983f.

[10] M. Li, T.-Y. Zhang, B. Xu, C.-Y. Hu, Z.-Y. Dong, Z. Wang, Y.-L. Tang, S.-L. Yu, Y. Pan, Q. Xian, Iodinated trihalomethanes formation in iopamidol-contained water during ferrate/chlor(am)ination treatment, Chemosphere 272 (2021), 129568, https://doi.org/10.1016/j.chemosphere.2021.129568.

[11] Z.-C. Gao, Y.-L. Lin, B. Xu, Y. Xia, C.-Y. Hu, T.-C. Cao, X.-Y. Zou, N.-Y. Gao, Evaluating iopamidol degradation performance and potential dual-wavelength synergy by UV-LED irradiation and UV-LED/chlorine treatment, Chem. Eng. J. 360 (2019) 806–816, https://doi.org/10.1016/j.cej.2018.12.022.

[12] X. Zhao, J. Jiang, S. Pang, C. Guan, J. Li, Z. Wang, J. Ma, C. Luo, Degradation of iopamidol by three UV-based oxidation processes: kinetics, pathways, and formation of iodinated disinfection byproducts, Chemosphere 221 (2019) 270–277, https://doi.org/10.1016/j.chemosphere.2018.12.162.

[13] Z.-Y. Dong, B. Xu, C.-Y. Hu, T.-Y. Zhang, Y.-L. Tang, Y. Pan, M. Gamal El-Din, Q.-M. Xian, N.-Y. Gao, The application of UV-C laser in persulfate activation for micropollutant removal: case study with iodinated X-ray contrast medias, Sci. Total Environ. 779 (2021), 146340, https://doi.org/10.1016/j.scitotenv.2021.146340.

[14] W. Wang, Z. Chen, Y. Zhou, P. Yan, J. Shen, S. Wang, J. Kang, J. Sun, Z. Wang, Y. Tong, Catalytic ozonation with silicate-based microfiltration membrane for the removal of iopamidol in aqueous solution, Sep. Purif. Technol. 257 (2021), 117873, https://doi.org/10.1016/j.seppur.2020.117873.

[15] Y. Cao, W. Qiu, J. Li, Y. Zhao, J. Jiang, S. Pang, Sulfite enhanced transformation of iopamidol by UV photolysis in the presence of oxygen: role of oxysulfur radicals, Water Res. 189 (2021), 116625, https://doi.org/10.1016/j.watres.2020.116625.

[16] Z. Dong, G. Chen, M. Li, F. Sun, C. Jiang, B. Bharti, Fe(II)-activated persulfate oxidation to degrade iopamidol in water: parameters optimization and degradation paths, Sci. Rep. 10 (1) (2020) 21548, https://doi.org/10.1038/s41598-020-78468-y.

[17] F.-X. Tian, W.-K. Ye, B. Xu, X.-J. Hu, S.-X. Ma, F. Lai, Y.-Q. Gao, H.-B. Xing, W.-H. Xia, B. Wang, Comparison of UV-induced AOPs (UV/Cl2, UV/NH2Cl, UV/ClO2 and UV/H2O2) in the degradation of iopamidol: Kinetics, energy requirements and DBPs-related toxicity in sequential disinfection processes, Chem. Eng. J. 398 (2020), 125570, https://doi.org/10.1016/j.cej.2020.125570.

[18] I. Sirés, E. Brillas, Remediation of water pollution caused by pharmaceutical residues based on electrochemical separation and degradation technologies: a review, Environ. Int. 40 (2012) 212–229, https://doi.org/10.1016/j.envint.2011.07.012.

[19] H. Dong, Z. Qiang, J. Lian, J. Li, J. Yu, J. Qu, Deiodination of iopamidol by zero valent iron (ZVI) enhances formation of iodinated disinfection by-products during

[20] chloramination, Water Res. 129 (2018) 319–326, https://doi.org/10.1016/j.watres.2017.11.032.

[20] S.O. Ganiyu, C.A. Martínez-Huitle, M.A. Rodrigo, Renewable energies driven electrochemical wastewater/soil decontamination technologies: a critical review of fundamental concepts and applications, Appl. Catal. B Environ. 270 (2020), 118857, https://doi.org/10.1016/j.apcatb.2020.118857.

[21] S. Cotillas, J. Llanos, I. Moraleda, P. Cañizares, M.A. Rodrigo, Scaling-up an integrated electrodisinfection-electrocoagulation process for wastewater reclamation, Chem. Eng. J. 380 (2020), https://doi.org/10.1016/j.cej.2019.122415.

[22] A.L. Schneider, S. Tisler, H. Schell, T. Matthée, B. Behrendt-Fryda, A. Tiehm, Electrochemical oxidation of iodinated X-ray contrast media by boron-doped diamond electrodes, Desalin. Water Treat. 91 (2017) 268–272, https://doi.org/10.5004/dwt.2017.20535.

[23] G. Del Moro, C. Pastore, C. Di Iaconi, G. Mascolo, Iodinated contrast media electrodegradation: process performance and degradation pathways, Sci. Total Environ. 506–507 (2015) 631–643, https://doi.org/10.1016/j.scitotenv.2014.10.115.

[24] M. Herraiz-Carboné, S. Cotillas, E. Lacasa, Á. Moratalla, P. Cañizares, M. A. Rodrigo, C. Sáez, Improving the biodegradability of hospital urines polluted with chloramphenicol by the application of electrochemical oxidation, Sci. Total Environ. 725 (2020), https://doi.org/10.1016/j.scitotenv.2020.138430.

[25] Á. Moratalla, D.M. Araújo, G.O.M.A. Moura, E. Lacasa, P. Cañizares, M.A. Rodrigo, C. Sáez, Pressurized electro-Fenton for the reduction of the environmental impact of antibiotics, Sep. Purif. Technol. 276 (2021), 119398, https://doi.org/10.1016/j.seppur.2021.119398.

[26] J.F. Pérez, J. Llanos, C. Sáez, C. López, P. Cañizares, M.A. Rodrigo, Development of an innovative approach for low-impact wastewater treatment: a microfluidic flow-through electrochemical reactor, Chem. Eng. J. 351 (2018) 766–772, https://doi.org/10.1016/j.cej.2018.06.150.

[27] I.M.D. Gonzaga, A. Moratalla, K.I.B. Eguiluz, G.R. Salazar-Banda, P. Cañizares, M. A. Rodrigo, C. Saez, Influence of the doping level of boron-doped diamond anodes on the removal of penicillin G from urine matrixes, Sci. Total Environ. 736 (2020), 139536, https://doi.org/10.1016/j.scitotenv.2020.139536.

[28] I.M. Kolthoff, E.M. Carr, Volumetric determination of persulfate in presence of organic substances, Anal. Chem. 25 (2) (1953) 298–301, https://doi.org/10.1021/ac60074a024.

[29] C.M. Dominguez, J. Parchão, S. Rodriguez, D. Lorenzo, A. Romero, A. Santos, Kinetics of lindane dechlorination by zerovalent iron microparticles: effect of different salts and stability study, Ind. Eng. Chem. Res. 55 (50) (2016) 12776–12785, https://doi.org/10.1021/acs.iecr.6b03434.

[30] M. Stieber, A. Putschew, M. Jekel, Reductive dehalogenation of iopromide by zero-valent iron, Water Sci. Technol. (2008) 1969–1975.

[31] A. Venkateshaiah, D. Silvestri, S. Wacławek, R.K. Ramakrishnan, K. Krawczyk, P. Saravanan, M. Pawlyta, V.V.T. Padil, M. Černík, D.D. Dionysiou, A comparative study of the degradation efficiency of chlorinated organic compounds by bimetallic zero-valent iron nanoparticles, Environ. Sci. Water Res. Technol. 8 (1) (2022) 162–172, https://doi.org/10.1039/D1EW00791B.

[32] F. Fu, D.D. Dionysiou, H. Liu, The use of zero-valent iron for groundwater remediation and wastewater treatment: a review, J. Hazard. Mater. 267 (2014) 194–205, https://doi.org/10.1016/j.jhazmat.2013.12.062.

[33] H. Dong, Z. Qiang, J. Lian, J. Li, J. Yu, J. Qu, Deiodination of iopamidol by zero valent iron (ZVI) enhances formation of iodinated disinfection by-products during chloramination, Water Res. 129 (2018) 319–326, https://doi.org/10.1016/j.watres.2017.11.032.

[34] J.W. Lee, D.K. Cha, Y.K. Oh, K.B. Ko, J.S. Song, Zero-valent iron pretreatment for detoxifying iodine in liquid crystal display (LCD) manufacturing wastewater, J. Hazard. Mater. 164 (1) (2009) 67–72, https://doi.org/10.1016/j.jhazmat.2008.07.147.

[35] S. Dbira, N. Bensalah, A. Bedoui, P. Cañizares, M.A. Rodrigo, Treatment of synthetic urine by electrochemical oxidation using conductive-diamond anodes, Environ. Sci. Pollut. Res. 22 (8) (2015) 6176–6184, https://doi.org/10.1007/s11356-014-3831-6.

[36] S. Cotillas, E. Lacasa, C. Sáez, P. Cañizares, M.A. Rodrigo, Removal of pharmaceuticals from the urine of polymedicated patients: a first approach, Chem. Eng. J. 331 (Supplement C) (2018) 606–614, https://doi.org/10.1016/j.cej.2017.09.037.

[37] S. Cotillas, E. Lacasa, M. Herraiz, C. Sáez, P. Cañizares, M.A. Rodrigo, The role of the anode material in selective penicillin G oxidation in urine, ChemElectroChem 6 (5) (2019) 1376–1384, https://doi.org/10.1002/celc.201801747.

[38] S. Cotillas, E. Lacasa, C. Sáez, P. Cañizares, M.A. Rodrigo, Electrolytic and electro-irradiated technologies for the removal of chloramphenicol in synthetic urine with diamond anodes, Water Res. 128 (2018) 383–392, https://doi.org/10.1016/j.watres.2017.10.072.

[39] M. Herraiz-Carboné, S. Cotillas, E. Lacasa, Á. Moratalla, P. Cañizares, M. A. Rodrigo, C. Sáez, Improving the biodegradability of hospital urines polluted with chloramphenicol by the application of electrochemical oxidation, Sci. Total Environ. 725 (2020), 138430, https://doi.org/10.1016/j.scitotenv.2020.138430.

[40] C.H. Jeong, E.J. Machek, M. Shakeri, S.E. Duirk, T.A. Ternes, S.D. Richardson, E. D. Wagner, M.J. Plewa, The impact of iodinated X-ray contrast agents on formation and toxicity of disinfection by-products in drinking water, J. Environ. Sci. 58 (2017) 173–182, https://doi.org/10.1016/j.jes.2017.03.032.

[41] S.D. Richardson, M.J. Plewa, To regulate or not to regulate? What to do with more toxic disinfection by-products? J. Environ. Chem. Eng. 8 (4) (2020), 103939 https://doi.org/10.1016/j.jece.2020.103939.

[42] T. Li, J. Farrell, Reductive dechlorination of trichloroethene and carbon tetrachloride using iron and palladized-iron cathodes, Environ. Sci. Technol. 34 (1) (2000) 173–179, https://doi.org/10.1021/es9907358.

[43] M. Stieber, A. Putschew, M. Jekel, Treatment of pharmaceuticals and diagnostic agents using zero-valent iron – kinetic studies and assessment of transformation products assay, Environ. Sci. Technol. 45 (11) (2011) 4944–4950, https://doi.org/10.1021/es200034j.

[44] C. Carvalho de Almeida, M. Muñoz-Morales, C. Sáez, P. Cañizares, C.A. Martínez-Huitle, M.A. Rodrigo, Integrating ZVI-dehalogenation into an electrolytic soil-washing cell, Sep. Purif. Technol. 211 (2019) 28–34, https://doi.org/10.1016/j.seppur.2018.09.065.

[45] Y. Bichsel, U. Von Gunten, Oxidation of iodide and hypoiodous acid in the disinfection of natural waters, Environ. Sci. Technol. 33 (22) (1999) 4040–4045, https://doi.org/10.1021/es990336c.